Symmetric, Isotopic Blends of Poly(dimethylsiloxane)

G. Beaucage,* S. Sukumaran, and S. J. Clarson

Department of Materials Science and Engineering, University of Cincinnati, Cincinnati, Ohio 45221

M. S. Kent and D. W. Schaefer

Organic Materials Division, Sandia National Laboratories, Albuquerque, New Mexico 87185

Received May 20, 1996; Revised Manuscript Received September 30, 1996[⊗]

ABSTRACT: Neutron scattering experiments were performed on three molecular weight pairs of symmetric, isotopic blends of poly(dimethylsiloxane) (PDMS) of near-critical composition. Scattering data covering close to 3 decades in size were globally fit using the random phase approximation (RPA) and the Debye function for Gaussian polymer coils using the interaction parameter, χ, and statistical segment length, b, as free parameters. These wide q range fits differ from the standard, narrow q range RPA fits in that the power-law scaling regime and exponential decay regimes, related to b, are accounted for. Values for χ showed a well-behaved linear dependence on inverse temperature. Critical temperatures were estimated from these data. Direct observations of the miscibility limit, through neutron cloud points, were made in several cases which agree to some extent with the extrapolated critical points. Monotonic dependencies in temperature of the coil expansion factor, α, as calculated from the statistical segment length, were observed. Under the assumption that the thermal dependence of α can be described in a Flory−Krigbaum form, this offers a second measure of the critical point in these blends. If coil expansion is accounted for in this way, the noncombinatorial entropic component of χ is observed to vanish in the high-molecular-weight limit in keeping with a Flory−Huggins/Hildebrand description of χ as B/T. The molecular weight dependence of χ supports the view that, after accounting for coil expansion, end-group effects are the sole source of noncombinatorial entropy in this model system.

Introduction

The random phase approximation (RPA) describes scattering from polymer blends in terms of the interaction parameter, χ, and the chain dimensions, chiefly the radius of gyration, R_g.[1] The RPA description should be applicable to Gaussian coils down to a size where Gaussian scaling succumbs to local, non-Gaussian features such as the persistence length or the screening length for interactions. In spite of this wide theoretical range of applicability in size, single-parameter data fits using the RPA approach are usually limited to a narrow range of size at low scattering vector, q, or large size. Inclusion of smaller size scattering data (higher q) generally leads to poor agreement between the RPA function and data as well as variability in the fit parameter, χ.[2−5] Several issues are important to this disagreement and the inability of the RPA function to fit scattering data over a wide range of q: (1) the local flexibility of the chain as reflected in the persistence length under the persistent chain model of Kratky and Porod;[3,6] (2) the range over which the screening of interactions plays a role in altering chain scaling under a blob or screening length model parallel to Edwards' description of semidilute solutions in good solvents;[7] (3) changes in large-scale (global) chain scaling, which is analogous to fractal model in nonequilibrium systems.[8] All three of these factors could lead to coil expansion, which is reflected in changes in R_g from the Θ value.

In order to explore these issues, a model system was investigated, isotopic blends of poly(dimethylsiloxane) (PDMS). PDMS displays coils with an unusually high degree of chain flexibility. This system is expected to yield good agreement with the RPA function using the Debye equation over a wide range of q because of this flexibility. Particularly, the third issue above, global deviation from Gaussian scaling, is expected to play no role in this system. Use of the RPA approach over a wide q range requires the use of an additional free parameter which reflects changes in the average size of the chains, the statistical segment length, b. This parameter can be equivalently expressed as a radius of gyration, as a characteristic ratio, or as a coil expansion factor, α. The last is preferable since the coil expansion factor is usually used to describe solvation effects and has a theoretical description in terms of temperature and molecular weight dependencies in dilute and semidilute solutions, which might be mimicked in polymer blends.

As noted above, PDMS has been used as an example of one of the simplest polymers since the Si−O bond is rotationally flexible. The situation is complicated by the polarity of the Si−O bond. Flory notes[9] that alternating bond angles in the PDMS chain and the ionic nature of the Si−O bond and perhaps the Si−C bond may lead to highly variable conformational behavior. A strong dependence of the unperturbed dimensions on solvent condition are observed in dilute solution for PDMS. The rotational flexibility of the Si−O bond is expected to lend true Gaussian statistics, on a large scale, under all conditions, in isotopic blends. PDMS is, additionally, the most highly compressible of conventional high polymers. Because of this, density effects might be expected to be apparent in this system if they are important to polymer miscibility.

A comprehensive study of miscibility in these blends has not been reported. Lapp, Picot, and Benoit[10] determined the interaction parameter, χ, for PDMS/d-PDMS at room temperature using a radius of gyration approach for the analysis of small-angle neutron scattering (SANS) data (extrapolation to zero concentration d-PDMS). In Lapp's work, blends of 6 and 0.9 number percent d-PDMS were investigated. The molecular

[⊗] Abstract published in *Advance ACS Abstracts,* November 15, 1996.

S0024-9297(96)00723-1 CCC: $12.00

weight of the d-PDMS was 267 kg/mol ($n_w = 3296$) and that of the PDMS was 14.6 kg/mol ($n_w = 195$), where n_w is the weight-average degree of polymerization. Polydispersities were close to 1.5 and were accounted for in the analysis. A critical composition for this blend was expected to be about 20% d-PDMS. The interaction parameter was calculated to be 1.7×10^{-3} at room temperature. Using $\chi n_{mean} = 2$ at the critical point, Lapp predicted that phase-separated blends will occur at room temperature for symmetric blends of about 100 kg/mol ($n_{mean} = 2600$), where n_{mean} is the average number of bonds in the main chain, i.e. $2\langle n_w \rangle$. This is very close to the experimental results discussed below. Upper critical solution temperature (UCST) behavior is generally observed for isotopic blends, although Lapp's work did not explore thermal variation of χ. The small difference in index of refraction between PDMS and d-PDMS precluded optical cloud point measurements.

All blends, reported here, were composed of equimolar ratios of the two isotopic components, and molecular weights within a blend pair were closely matched. The discussion below is largely restricted to this model system at critical composition. The random phase approximation (RPA),[1] using two free parameters, was used to determine the interaction parameter, χ, and the statistical segment length, b, directly from scattering data. Fits to the entire SANS data range, which covered close to 3 decades in q, were performed. This differs from RPA fits in the literature, which use only χ as a parameter and are performed over a narrow range of low q.

The RPA equation[1] describes the total scattered intensity or Rayleigh ratio, $R(q)$,[11] in terms of the scattering vector, $q = 4\pi/\lambda \sin(\theta/2)$, the radius of gyration of the polymer coil, R_g, and the site−site interaction parameter, χ.

$$R(q) = k_n[(z_A v_A \phi_A g_D(q,R_{gA}))^{-1} + (z_B v_B \phi_B g_D(q,R_{gB}))^{-1} - 2\chi/v_0]^{-1} \quad (1)$$

where $k_n = N_a(a_A/v_A - a_B/v_B)^2$, z_i is the degree of polymerization, ϕ_i is the volume fraction for a chain of type "i", v_i is the molar volume, a_i is the scattering length of a mer unit of type "i", and $v_0 = (v_A v_B)^{1/2}$.[12] N_a is Avogardo's number. The Debye equation, g_D, for a polymer coil describes scattering from a Gaussian chain,[13]

$$g_D(U) = 2(\exp(-U) - 1 + U)/U^2 \quad (2)$$

where $U = q^2R_g^2$. A simple test for the applicability of (2) in (1) is an observation of a power-law decay at intermediate q of slope −2.[8] R_g is generally expressed in terms of the degree of polymerization, n, and a scaling prefactor, b, the statistical segment length, $R_g^2 = nb^2/6$.

The scattering pattern generated by the RPA approach (1), using the Debye function (2) to describe Gaussian coils, leads to three general features in a log(intensity)−log(q) plot (cf. Figure 1). At low q, the pattern displays a constant value which will be affected, in part, by the value of the fit parameter $\chi(T,\phi,n)$. At intermediate q, the pattern displays an exponential decay whose position in q is governed by $U = q^2R_g^2$. At high q, a power-law decay of slope −2, mass fractal dimension of 2, with a prefactor of $2I(q=0,\chi=0)/R_g^2$ is generated.[8] Since only R_g appears in (1), and not b as an independent parameter, it is not possible to distinguish changes in the size of a statistical segment from changes in the number of statistical segments. In fact, since b is only a scaling prefactor, of limited physical significance, this is of minor consequence. Through consideration of the characteristic ratio, C_∞, or the coil expansion factor, α,[14] the reduced effect of an increase in R_g can be considered in common terms. The two parameters of (1) used to fit data in this paper, therefore, depend on different regimes of the scattering pattern in q. χ will affect $I(q=0)$, and R_g will affect the location in q of the exponential decay region and the power-law prefactor. Normally, the latter two features are largely ignored in application of (1) to small-angle neutron scattering data since only the lower q data are fit.

As noted, the RPA equation is generally used only at low q (cf. Figure 1), since it is difficult to obtain good fits over a wide range of q with a fixed b and because the thermodynamic parameter of interest, χ, is a global parameter that can best be measured at the largest accessible sizes or the lowest q. In the experiments presented here, data spanning a wide range of q were obtained at Los Alamos National Laboratory's LANSCE facility. Since PDMS displays an exceptionally flexible backbone, it was hoped to fit the Los Alamos data globally (over all available q) using the RPA equation to understand issues related to the limits of the applicability of the RPA approach and to see if coil expansion could account for unexpected dependencies of χ, as discussed below. The RPA approach requires a knowledge of the scaling behavior that relates the radius of gyration of a polymer coil to the molecular weight. Under a Gaussian model, as noted above, R_g is usually calculated from the degree of polymerization, n, using $R_g^2 = nb^2/6$, where b is a scaling prefactor called the statistical segment length. This scaling prefactor can be independently obtained in Θ solvents using light scattering, for example.[15] A value for b in PDMS of 5.61 Å is given in the literature.[9,14,16,17] This value had some agreement with the fit parameter for global fitting of the PDMS blends data, particularly for higher molecular weight blends near the miscibility limit. For the majority of the blends, an increase in b with temperature was observed, reflecting coil expansion. Coil expansion is usually expressed in terms of relative deviations from an ideal state as discussed below.[14]

The characteristic ratio, C_∞, is usually used to describe conformational effects under the Θ condition. The characteristic ratio at a finite molecular weight, C_M, can be calculated from the statistical segment length using

$$C_M = b^2/(2l^2) \quad (3)$$

where l, here, is the Si−O bond length of 1.64 Å. Flory[9] calculated the characteristic ratio for PDMS using a rotational isomeric states approach and found the characteristic ratio for PDMS to have a relatively wide accessible range (ref 9, p 177), reflecting the flexibility of Si−O bonds. Using the literature value for b, 5.61 Å, the characteristic ratio is 5.85 from (3). This value was used here to describe the unperturbed dimensions of PDMS.

The sensitivity of PDMS coils to solvent conditions is documented in the literature.[9] For example, in polar solvents a value of $C_\infty = 7.6$ has been reported (ref 14 and Table II-1 of ref 9). It is more appropriate to express this coil expansion in polar solvents in terms of the coil expansion factor, α,

$$\alpha^2 = C_{\text{measured}}/C_\infty \tag{4}$$

since α is traditionally used to account for solvation effects. For the polar solvent case, $\alpha = 1.14$. For semidilute solutions close to the overlap concentration, the coil expansion factor is related to the molecular weight and temperature through Flory−Krigbaum theory,[18,19]

$$\alpha^5 - \alpha^3 = K^* M^{1/2}\left(1 - \frac{\Theta}{T}\right) = KM^{1/2}\left(\frac{1}{2} - \chi\right) = A^* - B^*/T \tag{5}$$

where only the thermal dependence is accounted for in the latter expression. Equation 5 describes the scaling dependence of the coil expansion factor in terms of two constants, K^* and Θ, or, alternatively, K and $\chi(T)$. In (5), M is the number of steps in a Gaussian chain. A^* and B^* depend on the solvation condition and the number of interactions. Near the miscibility limit, at the theta temperature, Θ, the right side of (5) is zero due to the described thermal dependence and $\alpha = 1$. A^* and B^* are directly related to χ for semidilute solutions near the overlap concentration.

Flory−Huggins theory describes χ as a Hildebrand-type interaction parameter of the form B/T.[18] In polymer blends it is necessary to include an entropic component to χ, A, so that the thermal behavior of χ is given by

$$\chi = A + B/T \tag{6}$$

where the entropic term, A, is not accounted for in Flory−Huggins theory. The existence of A indicates a lapse in our understanding of miscibility in polymer blends and solutions. Several theories have attempted to account for this noncombinatorial entropy, for example using density changes under the equation of state theories.[20] The second function in (5) shows that good solvent conditions and coil expansion will occur when χ is less than $^1/_2$. The definition of χ, in terms of a Hildebrand approach, indicates that a positive χ reflects net repulsion between blend components in a linear sum of homogeneous and heterogeneous interactions in a binary blend considering site−site enthalpic interactions alone. Coil expansion and good solvent conditions are possible even with a weakly positive χ (i.e. χ positive but less than $^1/_2$) due to excluded volume, which is not considered in the Hildebrand definition of χ. That is, excluded volume drives coil expansion, which must be opposed by weakly repulsive site−site enthalpic interactions between blend components in order to obtain Gaussian scaling and $\alpha = 1$. This is important in explaining the existence of coil expansion in isotopic blends with no specific interactions where a weakly positive χ is expected *ab initio* in any reasonable model. Thus, we expect a weakly positive χ and $A = 0$ (eq 6) for true Flory−Huggins behavior in a model isotopic blend. True Flory−Huggins behavior, i.e. $A = 0$, has not been previously reported in the literature for polymer blends.

If coil expansion exists in polymer blends, it is expected that it will be negligible at several limits, the two composition limits, at the critical point, and at the spinodal. The parameters A^* and B^* are expected to depend on the molecular weight and the composition of the blend in ways not predicted by (5). The composition dependence of A^* and B^* will be such that they are negligible at the concentration limits, since the pure melts should be in the Θ condition. A^* and B^* should be maximum at the critical composition for a given molecular weight and temperature since the critical composition represents a maximum in solvation effects. The thermal dependence of (5) is expected to be obeyed in polymer blends if coil expansion is based on a balance of osmotic swelling and entropic contraction, as in Flory−Krigbaum theory. This thermal dependence yields a simple way to estimate the critical point for systems which display coil expansion. The applicability of this thermal dependence is discussed below, in relation to the blob/screening length model for coil expansion in polymer blends.

Gaussian scaling of polymer coils in a melt is a consequence of the screening of interactions over long distances. In the simplest terms, this screening prevents the expansion or contraction of the coil in a blend which otherwise might seem to be a logical consequence of changes in interactions with temperature and molecular weight. Scaling changes are known to occur in dilute and in semidilute solutions of polymers where screening is not complete. In the experiments discussed below, changes in R_g were observed with solvent condition. Additionally, there was clear evidence that Gaussian scaling was retained at intermediate scales (the power-law regime remains of -2 slope throughout the observed q). At least two models are possible to describe coil expansion while retaining global Gaussian scaling. (1) In analogy to semidilute solutions, local scaling changes might occur, such that at sizes below a screening length, good solvent scaling is present. This is termed the screening length or blob model here. A transition from Gaussian scaling, power law -2 in q, to good solvent scaling, a regime of $-^5/_3$ power law in q, is expected at extremely high q for this situation. Changes in solvent condition (i.e. temperature, composition, and molecular weight) would change the screening length in this model, thereby shifting the overall R_g. (2) Alternatively, the local conformation of the chains might be viewed as directly changing, leading to changes in the persistence length. For this model, a chemical reaction analogy has been proposed[3] for systems displaying specific interactions. For this persistent chain model, the Gaussian regime is expected to decay to a regime of -1 power law in q at the persistence length at highest q.

Unfortunately, in PDMS, these local deviatory scaling regimes occur at sizes out of range for the available data. However, the manifestation of these local conformational or scaling changes, in terms of coil expansion, can be investigated. Since the screening/coil expansion model has well-established expressions, (5), which describe the thermal behavior of α, this model can be explored in more detail. In considering coil expansion in polymer blends, the blob model of Edwards[7] for semidilute solutions is useful. This model is based on Gaussian scaling at large sizes, a transition at a length scale called the screening length, followed, in q, by good solvent scaling at smaller size scales until the persistence length is reached. The screening length defines a hypothetical construction termed a blob within which good solvent scaling exists. The Gaussian regime can be thought to statistically correspond to n_{blob} blobs arranged in a random walk configuration. n_{blob} is given by n_c/n^*, where n_c is the chain's degree of polymerization in terms of persistence lengths, l_{per}, and n^* is the number of persistence units in a hypothetical blob. The screening length, ξ, or blob size is given by $n^{*3/5} l_{\text{per}}$, reflecting good solvent conditions within a blob, where

Table 1. Characterization of Blend Components[a]

	15 kg/mol	25 kg/mol	75 kg/mol	300 kg/mol
deuterated mol wt	14	28.3	71.5	304
hydrogenous mol wt	16	25.8	71	303
deuterated DOP	189	381	964	4110
hydrogenous DOP	216	348	957	4080
deuterated M_w/M_n	1.02	1.06	1.05	1.1
hydrogenous M_w/M_n	1.02	1.05	1.06	1.1
critical $\chi = 2/n_{mean}$	0.00495	0.00274	0.00104	0.000244

[a] n_{mean} is twice the average degree of polymerization for a blend, i.e. the average number of bonds in the main chain.

l_{per} is the persistence length. The average end-to-end distance for the coil, R, is given by $n_{blob}^{1/2}\,\xi$, reflecting global Gaussian scaling at sizes above ξ under the blob model. The expansion factor, α, should depend directly on R and thus on $\xi^{1/6}$, since n_{blob} scales with $\xi^{-5/6}$. Thus, under the blob model,

$$\alpha = (\xi/l_{per})^{1/6} \tag{7}$$

Variability in solvation will change ξ and thereby α. Equation 7 can be used to estimate the q range for the scaling transition at ξ. If l_{per} is set roughly equal to the statistical segment length, 5.61 Å, and a value for α slightly larger than the maximum value observed here is used, $\alpha = 1.2$, then (7) predicts that the largest ξ is close to 17 Å. This is smaller than the minimum size observed in these experiments, 20 Å. Therefore, the blob approach is plausibly consistent with the data, presented below, which shows Gaussian scaling at all observed q (cf. Figure 1).

In contrast to Edwards' screening length approach, (5) describes uniform expansion of the coil at all size scales above the persistence length. If each blob is described by (5), then the thermal dependence of α will be retained globally. It should be emphasized that a blob does not exist as a discrete structure but rather as a construct to describe a transition in scaling at the screening length. This definition has parallels in the definition of a persistent unit by Kratky and Porod (ref 6 and Appendix G of ref 9). One problem with application of (5) to polymer blends is that the screening length defines the number of Gaussian steps, $M = n_{blob}$, under the screening length model. Alternatively, a variable persistence length will define the number of Gaussian steps in a persistent chain model. In either case, M is not constant with coil expansion since for global Gaussian scaling either the persistence length or the screening length will change with solvent conditions. Polymer blends, under either model, are not expected to obey the molecular weight dependence of (5) directly. The thermal dependence of (5), however, may be appropriate for polymer blends if the screening length model is correct.

To reiterate, for coil expansion to be reasonable, a local χ which is less than $^1/_2$ is necessary for good solvent conditions. A positive χ less than $^1/_2$ is consistent with net weak repulsive enthalpic interactions which are not strong enough to compensate for coil expansion due to excluded volume. The thermal dependence of (5) for α is expected, while the M dependence of (5) is not expected under a screening length/blob model for coil expansion in polymer blends.

Experimental Section

Table 1 lists the molecular weights of the blend components. PDMS and d-PDMS were synthesized anionically by a ring-opening mechanism followed by end-capping which resulted in trimethylsilane end groups.[21] All PDMS samples were viscous liquids and were mixed in a 50:50 molar ratio without solvents using a syringe. The samples were annealed at 50 °C in a vacuum oven for a week prior to the measurements. These samples were injected into 2 mm path length, spectroscopic grade, quartz cells. Incoherent and empty cell runs were subtracted from the scattering data to correct for background effects.

Scattering experiments were performed at the Los Alamos National Laboratories LANSCE facility and at the National Institute of Standards and Technology 8 m SANS beam line. Data from Los Alamos covered close to 3 decades in size. Data were converted to $R(q)$[11] in units of cm^{-1}. Conventionally, (1) is used to fit the first 10−20 data points of a data set covering more than 200 points (Figure 1). In such a local fit, the statistical segment length is fixed at the literature value. The scattering pattern over such a narrow range is not sensitive to coil expansion because the exponential knee and scaling regime are not fit. Since PDMS is an unusually flexible chain, displaying clear Gaussian scaling over a wide range of size and with a small persistence length, ≪10 Å, (1) should be theoretically applicable over the entire q range observed here. Scattering data were fit using a least-squares fitting routine with two free parameters, b and χ, using (1) and (2). Polydispersities of the two components were low and the polydispersity was not accounted for in the fits. The weight-average molecular weights were used to calculate the degree of polymerization. The statistical error from the data (cf. Figure 1) was propagated to all calculated and experimental results. This did not reflect other errors possible in the measurement such as composition, thickness, and temperature variability. Thickness was good to much less than a percent since uniform, quartz cells were used. Composition is good to about 1%. The error in the temperatures is close to ±0.1 °C.

The Los Alamos data were collected using a water/ethylene glycol bath for a heating stage. Temperatures from 0 to 98 °C were used on this apparatus. Sample temperatures were measured using a thermal probe at the sample and the values are good to about ±0.1 °C, as noted above. Samples were allowed to equilibrate for at least 0.5 h prior to measurements. At NIST, measurements well below room temperature were conducted using a cryostat. The temperature of the sample was assumed to match that of the cold finger, ±0.1 °C, to which they were attached. The cryostat operates under high vacuum, which led to experimental problems, chiefly the loss of some of the PDMS sample from the cell in some cases due to degassing of the PDMS. For these cases, it is believed that the NIST data are qualitatively correct while the absolute intensity is questionable due to some sample loss. In several cases, a sharp rise in the low-q intensity was observed in the neutron pattern on cooling the samples. This rise in low-q intensity was associated with macroscopic phase separation. In this regard, the relative intensity values from NIST proved quite useful in identifying the miscibility limit.

Results and Discussion

RPA fits were used to obtain χ and b as discussed above. A typical global fit to the RPA equation is shown in Figure 1. $R(q,T,\phi)$ is the Rayleigh ratio or absolute intensity and q is the scattering vector. As noted above, in this log−log plot a knee reflects a region of exponential decay that describes the radius of gyration. Linear regions reflect a power-law regime which describes the mass fractal scaling of the polymer chain.[3,22,23] In Figure 1, the power-law regime has a slope of −2 reflecting Gaussian statistics and a mass fractal dimension of 2. The fit in Figure 1 is good over a wide range of q, as occurred for all fits. In some cases, the statistical segment length varied considerably from the literature value in order to obtain global fits. The usual fit range for SANS data using (1) and a fixed b is also shown in Figure 1, as noted above. It is not possible to directly estimate ξ from the Gaussian regime since the definition of a fractal regime contains no account for small-scale features in this regime.

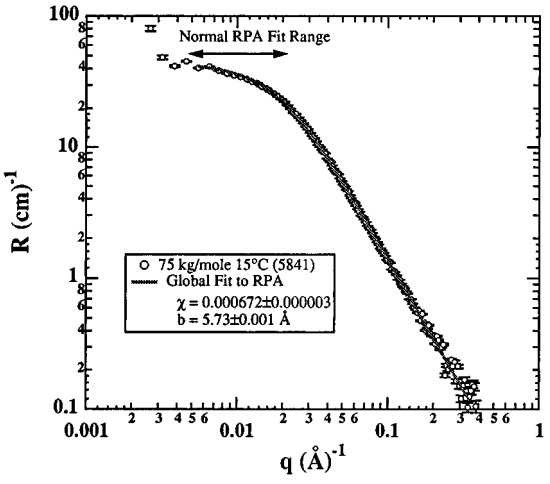

Figure 1. log−log plot of absolute intensity vs q for a 75 kg/mol symmetric, isotopic blend of PDMS at 15 °C. The values for the two free parameters in eq 1 are shown in the inset (Los Alamos data). Error bars indicate statistical error.

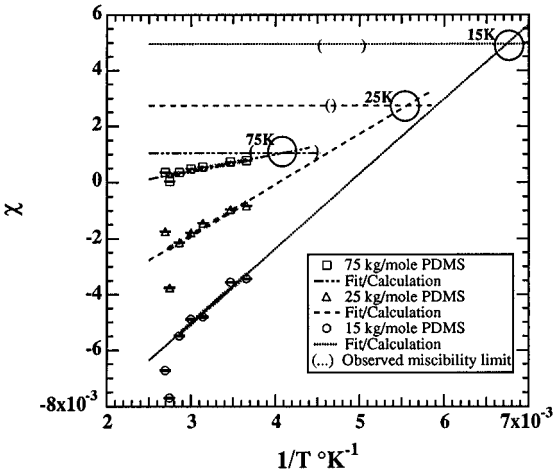

Figure 2. Values of χ and calculated critical χ plotted vs inverse temperature (Los Alamos data). Extrapolations to the critical point, where $\chi = \chi_{critical}$, yield the critical temperatures noted in the text. Fits are to (6).

Values obtained for χ, from fits similar to that of Figure 1, and calculated values for $\chi_{critical}$ are plotted against $1/T$ in Figure 2, following (6). The positive slope of χ versus $1/T$ indicates the presence of an upper critical solution temperature (UCST). (This was confirmed in neutron cloud point measurements mentioned below.) The horizontal lines in Figure 2 are calculated values for the critical χ using $2/n_{mean}$ from Table 1, where n_{mean} is twice the average degree of polymerization, reflecting the number of bonds in the main chain. Linear fits to the measured values using (6) are shown. Fits to (6) yield

$$\chi_{15} = -0.01304\ (\pm 0.00007) + 2.67\ (\pm 0.02)/T$$

$$\chi_{25} = -0.00727\ (\pm 0.00003) + 1.80\ (\pm 0.01)/T$$

$$\chi_{75} = -0.00135\ (\pm 0.00001) + 0.587\ (\pm 0.003)/T$$

where the subscript refers to the nominal molecular weight from Table 1. The indicated errors are propagated from the statistical errors in the data. All of the fits follow the functional form of (6). Using $\chi = 2/n_{mean}$, as shown in the figure, the line fits yield $T_{c15K} \approx -125 \pm 2$ °C, $T_{c25K} \approx -94 \pm 2$ °C, and $T_{c75K} \approx -28 \pm 2$ °C. The propagated statistical error reported for the 25K and 15K extrapolations does not completely reflect the experimental error involved in the extended extrapolation in Figure 2. The extrapolated critical temperatures do not agree with the observed cloud points for the 25K and 15K blends. This is discussed in detail below in relation to end-group effects. It should be noted that the higher molecular weight blend, with smaller end-group effects, yields a critical temperature which agrees with the observed miscibility limit.

Noncombinatorial entropy associated with coil expansion has been removed from these functions for χ since this was accounted for through the use of b as a fitting parameter. The small, negative A reported above, from (6), is believed to be due to the trimethylsilane end groups on the linear PDMS chains. The end-group effect serves to enhance miscibility since A is negative. One interpretation of this is that the randomization of end groups, not accounted for in the combinatorial entropy of Flory−Huggins theory, leads to this excess entropy term. B, from (6), is positive and small in all cases, indicating a net repulsive entropic interaction, which is expected in isotropic blends. From the values of B, a miscible regime at normal temperatures is supported and miscibility should be of the UCST type. As discussed below, the molecular weight dependence of A and B is consistent with simple end-group effects. Although negative values for χ are plotted in Figure 2, these negative values can be explained solely in terms of end-group effects.

The 300 kg/mol blend appeared to be phase separated at all accessible temperatures since the data could not be reasonably fit with (1) assuming a single phase. The results presented below indicate that the 300 kg/mol blend is immiscible at room temperature so mixing of miscible pairs was not achieved before the SANS experiments. Miscibilization of the 300 kg/mol blends would require an extended time at elevated temperatures using the reptation time as a basis.

End-group effects may play a role in the monotonic behavior of χ with molecular weight. All of the PDMS samples contain trimethylsilane end groups, as noted above, which might be expected to alter χ measurements. In terms of the A and B parameters of (6) for χ we expect

$$A = A_\infty + A'/n \tag{8a}$$

$$B = B_\infty + B'/n \tag{8b}$$

dependencies on molecular weight for end-group effects, where A_∞ and B_∞ are the extrapolated values for A and B in the absence of end groups (infinite molecular weight), A' and B' are the derivative values with respect to $1/n$ or the number density of end groups in terms of main-chain bonds, and n is the average degree of polymerization, i.e. $1/n = 2/n_{mean}$. Over the limited range of molecular weights studied, the parameters of (6) support the dependence of (8) (Figures 3 and 4). The linear fit for A fixes A_∞ to zero as expected from Flory−Huggins theory in the absence of nonconfigurational entropy due to end groups. A' in Figure 3, is -2.6 ± 0.6, indicating that the end groups are randomly distributed in the blend, thereby contributing to the entropy. The linear fit to B, Figure 4, shows a small positive intercept, $B_\infty = 0.15 \pm 0.1$, and a slope of 530 ± 100. Although these values must be viewed with care due to the limited number of molecular weights and the resulting large error, the small positive value for B_∞

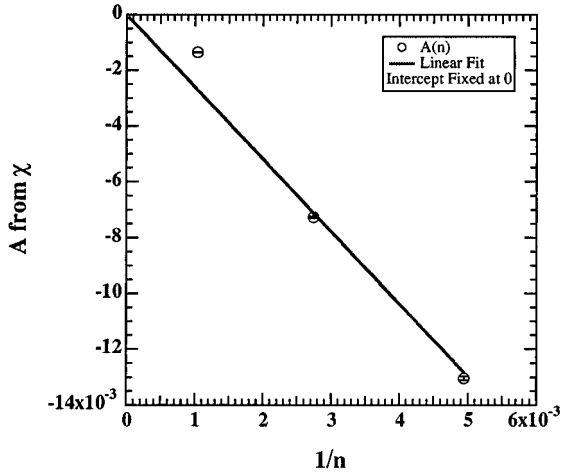

Figure 3. A ($\chi = A + B/T$, from fits of Figure 2) vs the inverse of the average degree of polymerization. Intercept in linear fit was fixed to 0.

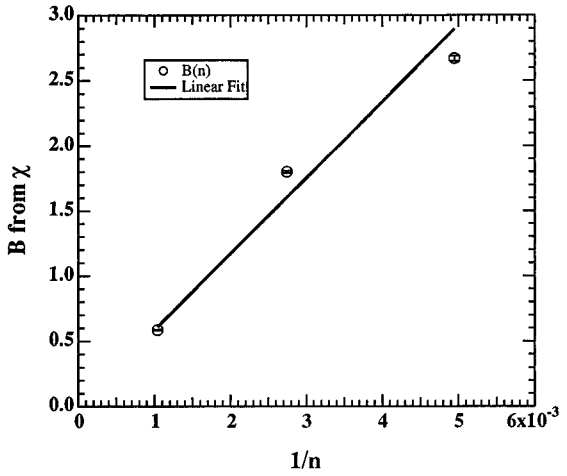

Figure 4. B ($\chi = A + B/T$, from fits of Figure 2) vs the inverse of the average degree of polymerization.

supports enthalpic interactions, in the absence of end groups, which are weak and repulsive, as might be expected for this isotopic system. B' is positive, indicating that the presence of end groups enhances the weak, repulsive enthalpic interaction between isotope pairs in this system. To reiterate, high-molecular-weight extrapolations of the χ function, with the inclusion of coil expansion in RPA fits for χ, supports true Flory–Huggins behavior with the residual noncombinatorial entropy and molecular weight dependence of B, consistent with an end-group effect.

In further measurements, performed at NIST, phase separation of these isotopic blends was observed as a rise in the low-q scattering coupled with a decrease in the high-q intensity that cannot be fit with the RPA approach under the assumption of a single phase. The rise in low-q intensity is related to the growth of large-scale domains that differ in neutron cross-section due to composition differences. High-q data reflect miscibility within these domains (reduction in intensity at high q). This is shown for the 15 kg/mol blend in Figure 5. The neutron cloud point, observed in this way, shows some agreement with extrapolated values from the Los Alamos data, as discussed below. The observed neutron cloud points were reversible. This was demonstrated by annealing phase-separated blends in the miscible regime. Scattering patterns from these annealed samples

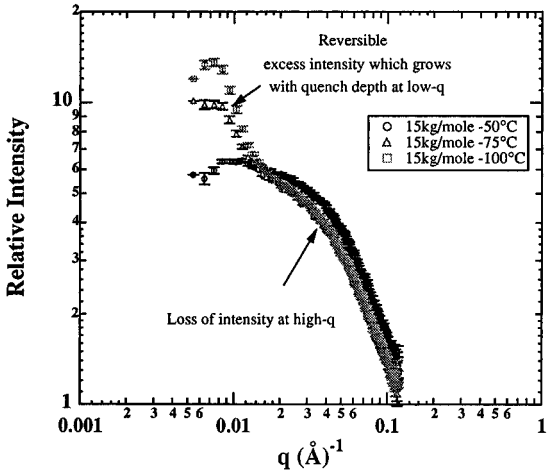

Figure 5. NIST data showing the growth of large-scale phases below the miscibility limit. log(relative intensity) vs log(q) are plotted. (Lowest two to three data points are corrupted by the beamstop.) Neutron cloud point is between −50 and −75 °C from these data. Estimate from Los Alamos data is $T_{c15K} \approx -125 \pm 2$ °C from Figure 2 and $T_{c15K} \approx -91 \pm 4$ °C from Figure 6.

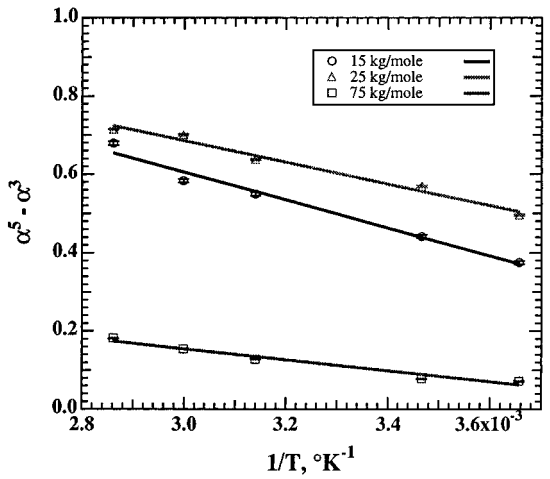

Figure 6. Coil expansion factor function from (5) vs inverse temperature for three PDMS blends. The temperature dependence indicates volumetric expansion of the PDMS coils with temperature. The linear-fit parameters are given in the text.

were identical to the initial runs before phase separation. The growth of large-size phases could then be repeated by lowering the temperature below the miscibility limit. The observed miscibility limit for the 15 kg/mol sample is between −50 and −75 °C. For the 25 kg/mol sample, the miscibility limit was observed between −55 and −60 °C. For the 75 kg/mol sample, the miscibility limit was observed between 0 and −50 °C. Low-temperature runs on the 300 kg/mol sample could not be fit using (1) and reasonable values for b, under the assumption of a single phase, indicating immiscibility at all temperatures below room temperature as noted above.

Figure 6 shows the behavior of the coil expansion factor, α, with temperature in terms of (5). α is calculated from fit values for b using (3) and (4), where the literature value of $C_\infty = 5.85$ was used. The thermal behavior of (5) agrees with the measured values in that a linear relationship is observed in inverse temperature. Linear fits yield the critical temperature where the extrapolated values of $\alpha^5 - \alpha^3$ go to 0. From (5)

$$(\alpha^5 - \alpha^3)_{15} = 1.67\ (\pm 0.02) - \frac{356\ (\pm 7)}{T}$$

$$(\alpha^5 - \alpha^3)_{25} = 1.51\ (\pm 0.01) - \frac{278\ (\pm 4)}{T}$$

$$(\alpha^5 - \alpha^3)_{75} = 0.573\ (\pm 0.008) - \frac{139\ (\pm 3)}{T}$$

where the subscripts, again, refer to the nominal molecular weight from Table 1. The molecular weight dependence of $\alpha^5 - \alpha^3$ is not monotonic in Figure 6 and differs strongly from the $M^{1/2}$ dependence predicted for dilute solutions. The linear fit parameters for the thermal dependence of $\alpha^5 - \alpha^3$, however, do show a monotonic behavior in molecular weight. Both A^* and B^* show a power-law dependence in N slightly weaker than -1 over the limited range of molecular weight and are not directly related to the fit values for χ from Figure 2, which is expected from dilute solution theory[9,10] (cf. (5)). This suggests that although coil expansion may be governed by a similar thermal mechanism as in good solvent theory for semidilute coils, the mechanism differs in detail. The tendencies of α are toward less expansion closer to the critical point in all cases. A possible explanation for this, using Edwards' blob model, is that the blob size is governed by solvent conditions. Better solvation leads to larger blobs and more expansion. A composition dependence is expected for $\alpha^5 - \alpha^3$ although it is not explored in these data. Since the pure melts should show no expansion, a maximum in blob size, and hence expansion, is expected at the critical composition.

There is some agreement between the observed miscibility limits and the extrapolated critical temperatures from Figures 2 and 6 (Figure 7). For the 15 kg/mol sample, the observed miscibility limit is between -50 and -75 °C while the extrapolated critical point, using $\alpha^5 - \alpha^3$, is -91 ± 4 °C; for 25 kg/mol, the observed miscibility limit is between -55 and -60 °C and the extrapolated critical temperature is -61 ± 7 °C; and for the 75 kg/mol blend, the miscibility limit is between 0 and -50 °C and the extrapolated critical point is -30 ± 8 °C. These calculated values show better agreement than those predicted by extrapolation of χ values from Figure 2; see Figure 7. All values for the miscibility limit agree, within the propagated error, for the higher molecular weight sample. Deviations from the observed miscibility limit grow monotonically larger with decreasing molecular weight. A larger molecular weight effect for the $\chi_{critical}$ extrapolation, relative to the $\alpha = 1$ extrapolation, might be expected since a stronger molecular weight dependence for χ relative to α was observed, as described below. The deviations between extrapolated and observed miscibility limits are probably due to end-group effects which are not described in either Flory–Huggins theory for χ or Flory–Krigbaum theory for α.

For the 300 kg/mol blend, the average degree of polymerization, n, is 4100 and an extrapolation of Figure 7 would indicate a miscibility limit at close to 120 °C with a large error. The highest temperature measured for the 300 kg/mol blend was 100 °C, and indication of immiscibility was observed for all temperatures as noted above.

Attempts to associate the thermal and molecular weight behavior of A^* and B^*, from the linear fits of Figure 6, with the observed dependencies of χ using the functional form of (5) were not successful. Resolution of this relationship awaits theoretical developments concerning the coil expansion behavior reported here. A^* and B^* do not clearly display the n^{-1} dependence which is supported for A and B from χ in Figures 3 and 4. An $n^{-1/2}$ dependence, which might be expected from (5) combined with this end-group effect, is also not supported by this limited range of molecular weights. The observed molecular weight dependence of A^* and B^* appears to be between these limits of $n^{-1/2}$ and n^{-1}.

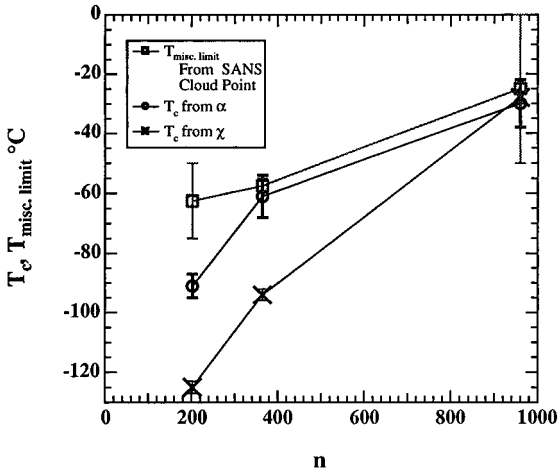

Figure 7. Extrapolated critical points from Figure 5 and 6 and observed miscibility limits using neutron cloud points as described in the text. n is the average degree of polymerization for the blend.

Summary

The RPA approach was used to fit scattering data from symmetric, isotopic blends of PDMS near the critical composition. Measurements were performed above 0 °C at Los Alamos and below 0 °C using a cryostat at NIST. The RPA equation was used to fit data over a much wider range of size than is conventionally done. This approach required the use of the statistical segment length as a free parameter, reflecting coil expansion in these critical composition blends. A qualitative observation of the miscibility limit was achieved in experiments at NIST using a cryostat. The Los Alamos data were extrapolated to the critical point, yielding critical temperatures that agreed to some extent with the observed miscibility limits.

Coil expansion was observed in all blends in that the statistical segment length, b, was larger than the Θ value of 5.61 Å. Using a Flory–Krigbaum functional form for the thermal dependency of the expansion factor, the critical point could be extrapolated from the observed dependence. The critical points obtained in this way showed agreement with the observed miscibility limits. The Flory–Krigbaum parameters did not show the square root of molecular weight dependence predicted for semidilute solutions near the overlap concentration. In fact, the molecular weight dependence of the Flory–Krigbaum parameters was to a weak negative power of M over the limited range observed. A composition dependence to coil expansion in polymer blends is also expected, although not explored here.

Although only three molecular weights over a limited range were investigated, speculation as to the molecular weight dependence of χ and α can be made. A model based on end-group effects for the entropic component of χ, A, is consistent with the data. For high-molecular-weight extrapolations, the inclusion of coil expansion

in RPA fits for χ supports true Flory−Huggins behavior, with the residual noncombinatorial entropy term being completely described in terms of end-group effects. These infinite molecular weight extrapolations also lead to a small positive enthalpic component to χ, B_∞, consistent with weak repulsive interactions in these isotopic blends. Since B_∞ is less than $^1/_2$, coil expansion is expected, from (5); that is, the small repulsive interaction is not enough to overcome excluded volume, which may drive coil expansion in this isotopic system. The molecular weight dependence of thermal expansion appears to be more complicated than this simple description of χ. Elaboration on the molecular weight dependence of α awaits further theoretical descriptions of coil expansion in polymer blends.

Acknowledgment. This work has benefited from the use of facilities at the Manuel Lujan, Jr. Neutron Scattering Center, a national user facility funded as such by the DOE/Office of Basic Energy Sciences. Phil Seeger and Rex Hjelm were of great assistance in performing the experiments. Results using the scattering facilities of the National Institute of Standards and Technology were conducted with the assistance of Charles Han, Charles Glinka, and Boulam Hamouda. The assistance of Charles Glinka in providing a cryostat for the low-temperature measurement is greatly appreciated. Some of this work was performed at Sandia National Laboratories, supported by the U.S. Department of Energy under Contract DE-AC04-94AL85000. Work at the University of Cincinnati was supported by a PRF-G grant from the American Chemical Society to G.B.

References and Notes

(1) de Gennes, P.-G. *Scaling Concepts in Polymer Physics*, Cornell University Press: London, 1979. Also, Hadziioannou, G.; Gilmer, J.; Stein, R. S. *Polym. Bull.* **1983**, *9*, 563. Jannik, G.; de Gennes, P.-G. *J. Chem. Phys.* **1968**, *48*, 2260. de Gennes, P.-G. *J. Phys. (Paris)* **1970**, *31*, 235. de Gennes, P.-G. *Faraday Discuss.* **1980**, *68*, 96.

(2) Yang, H. Ph.D. Dissertation, University of Massachusetts, Amherst, MA, 1986. Also: Shibayama, M.; Yang, H.; Stein, R. S. *Macromolecules* **1985**, *18*, 2179.

(3) Beaucage, G.; Stein, R. S. *Macromolecules* **1993**, *26*, 1617.

(4) Bates, F.; Wignall, G. *Macromolecules* **1986**, *19*, 934.

(5) Yang, H.; Stein, R. S.; Han, C. C.; Bauer, B.; Kramer, E. *Polym. Commun.* **1986**, *27*, 132.

(6) Porod, G. *Monatsh. Chem.* **1949**, *80*, 251. Also: Kratky, O.; Porod, G. *Recl. Trav. Chim. Pays-Bas* **1949**, *68*, 1106.

(7) Edwards, S. F. *Proc. Phys. Soc. London* **1966**, *88*, 265. Also: Doi, M.; Edwards, S. F. *The Theory of Polymer Dynamics*; Oxford Science Publications: New York, 1986. Also see ref 1, Chapter 3; Daoud, M.; Jannink, G. *J. Phys. (Paris)* **1976**, *37*, 973.

(8) Beaucage, G. *J. Appl. Crystallogr.* **1996**, *29*, 134.

(9) Flory, P. J. *Statistical Mechanics of Chain Molecules*; Interscience: New York, 1969; p 174.

(10) Lapp, A.; Picot, C.; Benoit, H. *Macromolecules* **1985**, *18*, 2437.

(11) The equivalence of the Rayleigh ratio common in light scattering measurements and the absolute intensity or cross section, $d\Sigma/d\Omega$, measured in neutron and X-ray scattering experiments was detailed by Higgins and Stein (Higgins, J. S.; Stein, R. S. *J. Appl. Crystallogr.* **1978**, *11*, 346. Also see: Russell, T. P.; Lin, J. S.; Spooner, S.; Wignall, G. D. *J. Appl. Crystallogr.* **1988**, *21*, 629.

(12) Joanny, J. F. *C. R. Acad. Sci., Paris* **1978**, *286B*, 89.

(13) Debye, P. Tech. Rep. 637 to Rubber Reserve Co., 1945; reprinted in: Debye, P. *The Collected Papers of Peter J. W. Debye*; Interscience: New York, 1954.

(14) A concise definition of these parameters is given in: Kurata, M.; Tsunashima, Y. In *Polymer Handbook*; Brandrup, J., Immergut, E. H., Eds.; John Wiley and Sons: New York, 1975; Chapter VII.

(15) A simple description of this approach is given in: Hiemenz, P. C. *Polymer Chemistry: The Basic Concepts*; Marcel Dekker Inc.: New York, 1984.

(16) Schultz, G. V.; Haug, A. *Z. Phys. Chem. (Frankfurt)* **1962**, *34*, 328.

(17) Lapp, A.; Strazielle, C. *Makromol. Chem., Rapid Commun.* **1985**, *6*, 591.

(18) Flory, P. J. *Principles of Polymer Chemistry*; Cornell University Press: London, 1953, p 600.

(19) Flory, P. J.; Krigbaum, W. R. *J. Chem. Phys.* **1950**, *18*, 1086.

(20) Sanchez, I. C. In *Polymer Blends*; Paul, D. R., Newman, S., Eds.; Academic Press: Orlando, 1978; Vol. I, Chapter 3.

(21) See: Chojnowski, J. In *Siloxane Polymers*; Clarson, S. J., Semlyen, J. A., Eds.; Ellis Horwood-PTR Prentice Hall: Englewood Cliffs, NJ, 1993; pp 23−40.

(22) Beaucage, G.; Schaefer, D. W. *J. Non-Cryst. Solids* **1994**, *17*, 2010.

(23) Beaucage, G. *J. Appl. Crystallogr.* **1995**, *28*, 717.

MA960723W